Received December 12, 2018, accepted December 18, 2018, date of publication December 26, 2018,
date of current version January 11, 2019.

Digital Object Identifier 10.1109/ACCESS.2018.2889721

Robust Adaptive Trajectory Linearization Control for Tracking Control of Surface Vessels With Modeling Uncertainties Under Input Saturation

BINGBING QIU, GUOFENG WANG, YUNSHENG FAN, DONGDONG MU, AND XIAOJIE SUN
Marine Electrical Engineering College, Dalian Maritime University, Dalian 116026, China

Corresponding author: Guofeng Wang (gfwangsh@163.com)

This work was supported in part by the Nature Science Foundation of China under Grant 51609033, in part by the Nature Science Foundation of Liaoning Province of China under Grant 20180520005, and in part by the Fundamental Research Funds for the Central Universities under Grant 3132018306 and Grant 3132016312.

ABSTRACT This paper develops a novel adaptive trajectory tracking control strategy to enhance the tracking performance for surface vessels with unmodeled dynamics and unknown time-varying disturbances. A high robustness and precision trajectory tracking controller is presented by using trajectory linearization control (TLC) technology, neural network, extended state observer (ESO), nonlinear tracking differentiator, and auxiliary dynamic system. First, the greatest advantage of this paper is that the TLC technology is first introduced into the field of surface vessels motion control, which provides a new direction for TLC technology research. Then, to further enhance the control performance and robustness of the system, the neural network with minimum learning parameter is used to replace the classical radial basis function neural network to approximate unmodeled dynamics, which can reduce the burden of computing. A novel reduced-order ESO is constructed to estimate unknown time-varying disturbances to achieve real-time compensation. Meanwhile, nonlinear tracking differentiator is employed to realize the derivative of virtual control command, as well as to provide command filtering. In addition, an auxiliary dynamic system is designed to reduce the risk of actuator saturation. The stability of the closed-loop system is guaranteed based on the Lyapunov criteria. Lastly, the comparison results demonstrate the superior performance of the proposed approach.

INDEX TERMS Trajectory linearization control, surface vessels, neural network, auxiliary dynamic system, extended state observer, nonlinear tracking differentiator.

I. INTRODUCTION

With the rapid development of ocean techniques, marine vessels have been widely utilized in the sea for several major tasks, such as marine transportation, the oil and gas exploration, rescue operations [1]–[3]. In the practical engineering, trajectory tracking control is not only the basis of all tasks but also the key to ensure navigation safety. However, the tracking performance is significantly decreased due to the effects of the environment. Therefore, enhancing the tracking control of surface vessels, has been significant and attracted a lot of attention from both industrial and academia.

Focusing on the surface ships motion control, many effective control algorithms have arose in the control system. Initially, based on model-free control methods, a proportional integral derivative (PID) controller is designed in [4], and an intelligent control method based on the fuzzy logic is developed in [5]. However, both methods have low precision of tracking performance because model-free control methods are easily affected by environmental factors. To improve tracking performance, model-based control methods have been developed. Some control methods such as backstepping control [6] and model predictive control [7] have been developed to design trajectory tracking controller. However, these methods have large offset errors with the increase of the model uncertainty and disturbance. To further improve tracking performance, some of adaptive robust control algorithms have been developed in [8]–[11], which can suppress all random uncertainties in the drive and response system. Combining the average dwell-time scheme and the adaptive backstepping technology, the paper [12] proposes an adaptive neural state-feedback controller for a class of nonlinear switched systems, in which radial basis function (RBF) neural network is adopted to approximate uncertainty factors. Based on the dynamic surface control method, an adaptive neural-network control method is developed in [13], where an appropriate state observer is designed to estimate the unmeasured state. In [14], an adaptive robust coupling control approach is presented for offshore crane system, which can handle unknown disturbances and uncertain parameters. The paper [15] develops a practical adaptive robust controller based on extended state observer subject to the unstructured and structured uncertainties, in which a feedforward cancellation technique is used to compensate for unmodeled dynamics and external disturbances. The advantage of the above work is that the adaptive control methods have good control performance and robustness. In addition, trajectory linearization control (TLC) technology is a nonlinear tracking and decoupling control method, which consists of nonlinear dynamic inversion and a linear time-varying (LTV) feedback stabilization. Compared with the other methods, it has not only a simple structure but also enough anti-interference and robustness. Therefore, TLC technology has been successfully applied to the controlling of missiles [16], X-33 flight [17], helicopter [18] and aircraft [19]. However, TLC technology can only achieve local exponential stability, and it has never been applied in the field of surface ships motion control.

To cope with model uncertainty and disturbance, considerable researches have been conducted to investigate and address the above in [20]–[28]. The first methodology for eliminating system uncertainties is robust control technique and learning technique. First, sliding mode control (SMC) [20] is a well-known robust control technique, but the chattering problem affects the control performance of the control system. In [21], integral sliding mode control has been developed, where the matched unmodeled dynamics and unknown time-varying disturbances can be compensated online, while the unmatched disturbances will not be amplified. Learning techniques based on neural network or fuzzy logic have been widely used to handle uncertainties of system [22], [23]. However, the fuzzy logic requires experience or prior knowledge to provide system design, for simple fuzzy processing of information, which will lead to the reduction of control accuracy and dynamic quality deterioration of the system. Therefore, in the actual controller design, the application of neural network is more extensive than fuzzy logic for solving unmodeled dynamics and unknown time-varying disturbances. The second methodology is to estimate and compensate the disturbances by using observers including extended state observer (ESO) [24]–[26], sliding-mode disturbance observer (SMDO) [27] and extended disturbance observer (EDO) [28]. The main design idea is to estimate the uncertainty of the unknown first. Then, the estimated system uncertainty is fed back to the controller to compensate for the uncertainty. In addition, to get closer to practical engineering, input saturation [3], [29], [30] is considered in the design of the controller, which is an unavoidable problem due to the physical limitations of the propulsion system. In other words, the commanded control inputs calculated by the trajectory tracking controller may exceed the limitation of the maximum force and moment, which will lead to instability of the system. The existence of input saturation not only affects the performance of the controller but also relates to the security of the trajectory tracking. Hence, it is very important to solve the problem of input saturation for the design of trajectory tracking controller.

In this paper, motivated by the existing results, taking into account actuator saturation, unmodeled dynamics and unknown time-varying disturbances, a novel robust adaptive control controller is performed according to TLC technology, neural network, reduced-order ESO and auxiliary dynamic system, which makes surface vessels track a specific trajectory accurately. The following summarizes the main contributions of this paper:

(1) TLC technology has been proven to be an effective control technique, which is further developed by introducing TLC into the field of ship motion control. Through the author's view, it is used for the first time in the design of trajectory tracking controller for surface vessels.

(2) Taking full account of practical engineering, an auxiliary dynamic system is introduced into tracking controller design to handle the risk of actuator saturation. In addition, both unmodeled dynamics and unknown time-varying disturbances can be estimated by constructing neural network with minimum learning parameter (MLP) and reduced-order ESO, respectively. The main advantage is that neural network MLP replaces RBF neural network to reduce the computational burdens, leading to improved optimizing efficiency.

(3) A practical robust trajectory tracking control law in forms of PI is proposed, and suggestions for adjusting control parameters are given in this paper. In two cases, the simulation results confirm the superior performance of the proposed strategy.

The paper is organized as follows. In Section 2, system model and preliminaries are introduced. In Section 3, a novel trajectory tracking control scheme for surface vessels is designed. Section 4 gives the stability of the system. Simulation results and comparisons are considered in Section 5. Section 6 concludes this article and introduces future research.

II. SYSTEM MODEL AND PRELIMINARIES

A. MODELING OF SURFACE VEHICLE

In this section, the earth-fixed frame and the body-fixed frame are employed to study the model of surface vessel. In Fig. 1, $O - X_0Y_0Z_0$ is the earth-fixed inertial frame $\{i\}$ and $o - x_0y_0z_0$ is the body-fixed frame $\{b\}$. In actual navigation, surface vessel consists of 6 DOFs: the surge velocity u, sway

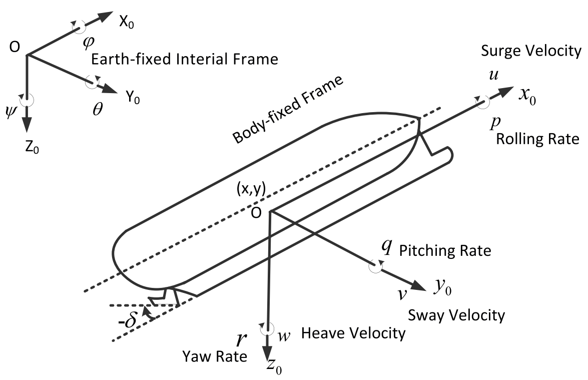

FIGURE 1. **The earth-fixed inertial and the body-fixed frame.**

velocity v, heave velocity w, yaw rate r, rolling rate p and pitching angle q, respectively. However, only the horizontal movement of surface vessel is considered in this paper. Therefore, the heave velocity, rolling rate and pitching angle are ignored. The position and orientation in $\{i\}$ are expressed as $\eta = [x, y, \psi]^T$ and surge speed, sway speed and yaw rate in $\{b\}$ are expressed as $\upsilon = [u, v, r]^T$.

From the above analysis, the nonlinear mathematical model of 3DOFs ship motion can be expressed as [31]

$$\dot{\eta} = J(\psi)\upsilon \tag{1}$$

$$M\dot{\upsilon} + C(\upsilon)\upsilon + D\upsilon = \tau + \Xi(\upsilon) + b(t) \tag{2}$$

where

$$J(\psi) = \begin{bmatrix} \cos(\psi) & -\sin(\psi) & 0 \\ \sin(\psi) & \cos(\psi) & 0 \\ 0 & 0 & 1 \end{bmatrix}$$

is the rotation matrix from $\{b\}$ to $\{i\}$. $M = diag(m_{11}, m_{22}, m_{33})$ is the inertial matrix including added mass, $C(\upsilon) \in R^{3\times 3}$ is the Coriolis and Centripetal matrix that can be derived from M;

$$D = \begin{bmatrix} d_{11} & 0 & 0 \\ 0 & d_{22} & d_{23} \\ 0 & d_{32} & d_{33} \end{bmatrix}$$

is the hydrodynamic damping matrix; $\tau = [\tau_1, \tau_2, \tau_3]^T$ denotes the control forces and moment; $\Xi(\upsilon) \in R^3$ and $b(t) \in R^3$ are unmodeled dynamics and unknown time-varying disturbances, respectively.

Control objective: Under the influence of the unmodeled dynamics and unknown time-varying disturbances, the surface vessel can track the reference path (x_d, y_d, ψ_d) accurately by the design of the controller τ.

Remark 1: In general, $b(t)$ is much lower in frequency than ship dynamics. In addition, due to nonlinear tracking differentiator, the high-frequency interference has been removed before entering the kinematics and kinetic control loop. Therefore, unknown disturbance $b(t)$ can be regarded as slow time-varying [32].

Assumption 1: The reference path or trajectory of the target is regular and smooth enough, x_d, $\dot{x}_d$, y_d, $\dot{y}_d$, ψ_d and $\dot{\psi}_d$ are all bound.

Assumption 2: The unmodeled dynamics and external disturbances accord with the following assumption: $\|\Xi\| \leq \Xi_{\max}$, $\|b\| \leq b_{\max}$, where $\Xi_{\max}$ and $b_{\max}$ are unknown positive constants.

B. TLC TECHNOLOGY

In order to facilitate the design of TLC controller, the kinetic equation (2) can be written as a form of nonlinear feedback

$$\dot{\upsilon} = F_1(\upsilon) + G_1(\upsilon)\tau + G_3(\upsilon)\Xi(\upsilon) + G_2(\upsilon)d(t) \tag{3}$$

where $F_1(\upsilon) = -M^{-1}(C(\upsilon)\upsilon + D\upsilon)$, $G_1(\upsilon) = M^{-1}$, $G_2(\upsilon) = G_3(\upsilon) = diag(1, 1, 1)$, $\Xi(\upsilon) = \theta M^{-1}F_1(\upsilon)$, $\theta = diag(\theta_u, \theta_v, \theta_r)$ is an unmodeled degree coefficient, and $d(t) = M^{-1}b(t)$ represents unknown time-varying disturbances. In addition, there exist three nonlinear matrixs $G_0(\upsilon)$, $G_4(\upsilon)$ and $G_5(\upsilon)$, which satisfy

$$\begin{aligned} G_1(\upsilon)G_0(\upsilon) &= G_2(\upsilon) \\ G_1(\upsilon)G_4(\upsilon) &= G_3(\upsilon) \\ G_2(\upsilon)G_5(\upsilon) &= G_3(\upsilon) \end{aligned} \tag{4}$$

First, without consideration of $d(t)$ and $\Xi(\upsilon)$, $\upsilon^*$and $\bar{\tau}$ are the nominal state and nominal input, respectively. Then the nominal trajectory satisfies

$$\dot{\upsilon}^* = F_1\left(\upsilon^*\right) + G_1\left(\upsilon^*\right)\bar{\tau} \tag{5}$$

Define the kinetic loop tracking error $E_2 = \upsilon - \upsilon^*$, without considering input saturation, the control law of TLC technology is proposed as

$$\tau_0 = \bar{\tau} + \tilde{\tau} \tag{6}$$

where $\tilde{\tau}$ represents the LTV feedback control law.

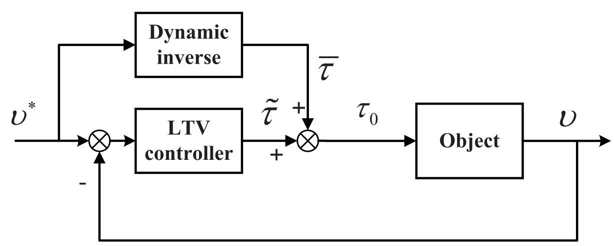

FIGURE 2. **TLC scheme diagram.**

Obviously, the original TLC controller consists of two components, as shown in Fig. 2.

(1) A dynamic inverse controller that generates the nominal control input $\bar{\tau}$.

(2) The LTV feedback control law $\tilde{\tau}$ is designed to handle unknown model dynamics and time-varying disturbances, which can stabilize the LTV system and have a certain response characteristics.

The differential of E_2 can be written as

$$\begin{aligned}\dot{E}_2 &= \dot{\upsilon} - \dot{\upsilon}^* \\ &= F_1(\upsilon) + G_1(\upsilon)\tau - F_1(\upsilon^*) - G_1(\upsilon^*)\bar{\tau} \\ &= F_1(\upsilon^* + E_2) + G_1(\upsilon^* + E_2)(\bar{\tau} + \tilde{\tau}) \\ &\quad - F_1(\upsilon^*) - G_1(\upsilon^*)\bar{\tau} \\ &= f_2(\upsilon^*, \bar{\tau}, E_2, \tilde{\tau}) \end{aligned} \tag{7}$$

where υ^* and $\bar{\tau}$ can be regarded as two time-varying parameters, (7) can be rewritten as

$$f_2(\upsilon^*, \bar{\tau}, E_2, \tilde{\tau}) = f_2(t, E_2) \tag{8}$$

By linearizing (8) along $(\upsilon^*, \bar{\tau})$, we have

$$\dot{E}_2 = A_2(t)E_2 + B_2(t)\tilde{\tau} \tag{9}$$

where $A_2(t) = \left(\frac{\partial F_1}{\partial \upsilon} + \frac{\partial G_1}{\partial \upsilon}\tau\right)|_{\upsilon^*,\bar{\tau}}$, $B_2(t) = G_1|_{\upsilon^*,\bar{\tau}}$. The system (8) and (9) satisfy the following Assumptions:

Assumption 3: Let $E_2 = 0$ be an isolated equilibrium point for (8), and $F : [0, \infty) \times D_E \to \mathbb{R}^n$ can be continuously differentiable, among which $D_E = \{E_2 \in \mathbb{R}^n \, \|E_2\| < R_e\}$. The Jacobian matrix $[\partial F/\partial E_2]$ is a bounded and Lipschitz on D_E, uniformly in t [33]–[35].

Assumption 4: $(A_2(t), B_2(t))$ is uniformly completely controllable for the system (9).

The LTV feedback control law can be designed by the differential algebraic spectrum theory [36], [37], which can be expressed as

$$\tilde{\tau} = K_2(t)E_2 \tag{10}$$

From [33], the system (8) maintains exponential stability at $E_2 = 0$. Hence, we have

$$A_c(t) = A_2(t) + B_2(t)K_2(t) \tag{11}$$

where A_c is Hurwitz, it makes the system (11) asymptotically stable.

However, in the actual tracking process, $d(t)$ and $\Xi(\upsilon)$ always exist. Hence, when $d(t)$ and $\Xi(\upsilon)$ are taken into account in design controller, (8) can be redefined as

$$\dot{E}_2 = f_2(t, E_2) + G_3(\upsilon)\Xi(\upsilon) + G_2(\upsilon)d(t) \tag{12}$$

From the above structure, the state error stabilization for the system (12) has been transformed into the problem of unmodeled dynamics and external disturbance rejection. However, the original TLC technology can only achieve local exponential stability, with the increase of $\|G_3(\upsilon)\Xi(\upsilon) + G_2(\upsilon)d(t)\|$, the performance of TLC technology is reduced or invalid.

C. NEURAL NETWORK MINIMUM LEARNING PARAMETER METHOD

Neural network has a powerful approximation ability, especially RBF neural network has been widely used to solve the problems of unknown model dynamics [38]. In this paper, neural network MLP replaces RBF neural network to compensate for unmodeled dynamics, which can reduce the complexity of the calculation.

RBF neural network is three-layer forward, consisting of input layer, hidden layer, output layer. The output of RBF neural network can be written as

$$F(Z) = W^T\Theta(Z) + \varepsilon \tag{13}$$

where Z and $F(Z)$ are the input and output of the RBF neural network, respectively. $W \in \mathbb{R}^{n\times l}$ is the weight matrix of the hidden nodes, and $\Theta(Z)$ is the Gaussian function of the hidden nodes. $\varepsilon \in \mathbb{R}^n$ is an approximation error vector with bound. From [39], $\|\varepsilon\| \leq \bar{\varepsilon}$, $\bar{\varepsilon}$ is an unknown positive number.

However, from the parameter adaptation law of RBF neural network in [40]–[42], all weight vectors require real-time online learning, which undoubtedly increases the complexity of the calculation. On the other hand, it is also not easy to practice in ship control engineering. Therefore, in order to reduce the computational complexity, RBF neural network is replaced by neural network MLP to approximate unmodeled dynamics [43]. The principle is that adaptive neural network is employed, in which the weight's updating law is simplified by using the Young's inequality. More exactly, $\Phi = \|W\|^2$, and $\hat{\Phi}$ is the estimate of Φ. The estimation error is $\tilde{\Phi} = \hat{\Phi} - \Phi$.

D. IN SATURATION

Input saturation is a common and difficult problem in trajectory tracking controller design, and its existence strongly affects the control performance of the system. If the output of the designed controller exceeds the maximum value of the propulsion system, it may cause system instability or crash. Therefore, in order to improve the design performance of the controller, an auxiliary dynamic system is constructed to deal with input saturation in this paper.

First, in practice, due to physical limitations of the propulsion system, the control force and moment are limited, which is represented as

$$\tau_i = \begin{cases} \tau_{i\max}, & \text{if } \tau_{oi} > \tau_{i\max} \\ \tau_{oi}, & \text{if } \tau_{i\min} < \tau_{oi} < \tau_{i\max} \\ \tau_{i\min}, & \text{if } \tau_{oi} < \tau_{i\min} \end{cases} \tag{14}$$

where $\tau_{i\max}$ and $\tau_{i\min}$ $(i = 1, 2, 3)$ are the maximum and minimum output, $\tau_o = [\tau_{o1}, \tau_{o2}, \tau_{o3}]^T$ is the command calculated by the tracking controller.

In order to handle input saturation (14), an auxiliary dynamic system [44] is designed as

$$\dot{\zeta} = \begin{cases} -K_\zeta\zeta - \dfrac{\sum_{i=1}^{3}|\mu_i\Delta\tau_i| + 0.5\Delta\tau^T\Delta\tau}{\|\zeta^2\|}\cdot\zeta + \Delta\tau, & \|\zeta\| > \sigma \\ 0_{3\times 1}, & \|\zeta\| < \sigma \end{cases} \tag{15}$$

where $\zeta = [\zeta_1, \zeta_2, \zeta_3]^T$ is the state vector of the system, $K_\zeta = K_\zeta^T \in R^{3\times 3}$ is a positive definite design matrix. μ_i is an error

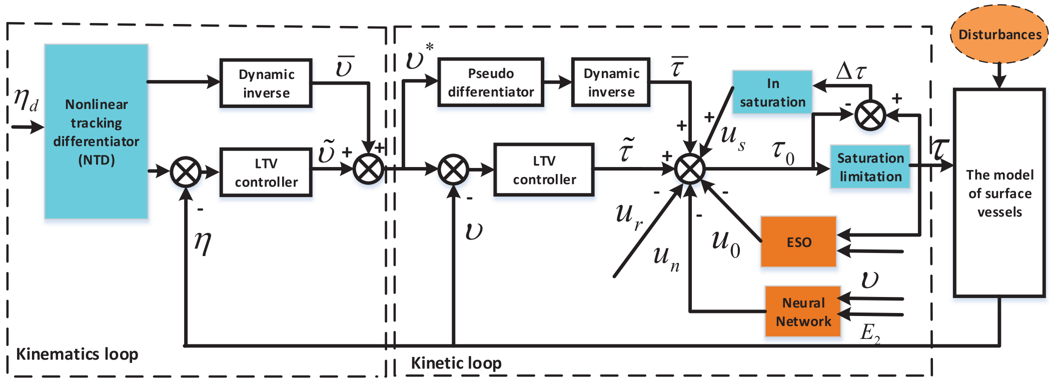

FIGURE 3. The structure of the proposed trajectory tracking control scheme for surface vessels.

variable, and $\Delta\tau = \tau - \tau_o$. In addition, $\sigma > 0$ is a small parameter, and $\dot{\zeta} = 0_{3\times 1}$ can avoid the singularity problem when $\|\zeta\| < \sigma$.

III. CONTROL DESIGN

A. STRUCTURE OF THE PROPOSED CONTROL SCHEME

Fig. 3 demonstrates the structure of the proposed novel trajectory tracking control scheme for surface vessels with unmodeled dynamics and unknown time-varying disturbances. It mainly consists of two parts: the kinematic loop and kinetic loop. The kinematic loop controller can track the given command filtered by NTD. The kinetic loop controller can track the virtual command produced by the pseudo differentiator. The designed TLC controller consists of pseudo-dynamic inverse controller (open-loop control) and a LTV controller (close-loop control). In addition, the problem of the input saturation is solved by designing an auxiliary dynamic system. Meanwhile, to improve the robustness and control performance of the system, the neural network MLP and reduced-order are applied to achieve online estimation and compensation for unmodeled dynamics and unknown time-varying disturbances, respectively. Finally, in order to further improve the tracking performance of the system, adaptive robust control term is designed to overcome the influence of approximation error of the system.

B. NONLINEAR COMPOSITE CONTROLLER DESIGN

1) KINEMATICS CONTROL LOOP

First, the main task of this section is to design a control law to track the reference η_d. According to the structure of TLC, the nominal input (without uncertainties) can be obtained by inverting (1) as

$$\bar{\upsilon} = J\left(\psi_d^*\right)^{-1}\dot{\eta}_d^* \tag{16}$$

where the symbol $\bar{\upsilon}$ denotes nominal kinematics controller, $\dot{\eta}_d^*$ is obtained by the η_d through the second-order linear differentiator (SOLD).

In the traditional TLC design, SOLD is used to produce η_d^* and $\dot{\eta}_d^*$ by the nominal input η_d, which has been used in many controller designs [17]–[19]. SOLD is expressed as follows

$$\begin{cases} \dot{z}_1 = z_2 \\ T_m\dot{z}_2 = -(z_1 - \eta_d) - 2T_m z_2 \\ y = z_2 \end{cases} \tag{17}$$

where T_m is the time constant.

It is obvious that $\lim\limits_{T_m\to 0} z_1 = \eta_d = \eta_d^*$, $\lim\limits_{T_m\to 0} z_2 = \dot{\eta}_d = \dot{\eta}_d^*$. When the initial conditions of $z_1(0)$ and $\eta_d(0)$ have large errors, due to the high gain influence of the differentiator, the derivative of $\eta_d(0)$ will produce a peak phenomenon near the initial time. Even nominal differential signal $\dot{\eta}_d^*$ and input $\bar{\upsilon}$ also have signal hopping, which will lead to the saturation of the control input instantaneously. In the traditional TLC technology, it can be seen that the peak phenomenon is unavoidable. To solve the above problems, a nonlinear tracking differentiator (NTD) is introduced into this paper to replace SOLD. In [45], the specific form of NTD is expressed as

$$\begin{cases} fh = fhan\left(\eta_d^*(k) - \eta_d(k), \dot{\eta}_d^*(k), r_1, h_1\right) \\ \eta_d^*(k+1) = \eta_d^*(k) + h_1 \cdot \eta_d^*(k) \\ \dot{\eta}_d^*(k+1) = \dot{\eta}_d^*(k) + h_1 \cdot fh \end{cases} \tag{18}$$

where h_1 and r_1 denote the sampling period and acceleration factor, respectively. In NTD, the peak of the differential signal is regulated by acceleration factor r_1. Therefore, it can avoid the peak phenomenon in linear differentiator.

Define the kinematic loop tracking error $E_1 = \left[x - x_d^*\ y - y_d^*\ \psi - \psi_d^*\right]^T = \left[e_x\ e_y\ e_\psi\right]^T$, by linearizing (1) along the nominal $\left(\eta_d^*, \bar{\upsilon}\right)$, we have

$$\begin{bmatrix} \dot{e}_x \\ \dot{e}_y \\ \dot{e}_\psi \end{bmatrix} = A_1(t)\begin{bmatrix} e_x \\ e_y \\ e_\psi \end{bmatrix} + B_1(t)\underbrace{\begin{bmatrix} \tilde{u} \\ \tilde{v} \\ \tilde{r} \end{bmatrix}}_{:=\tilde{\upsilon}} \tag{19}$$

where

$$A_1(t) = \begin{bmatrix} 0 & 0 & -\sin\left(\psi_d^*\right)\bar{u} - \cos\left(\psi_d^*\right)\bar{v} \\ 0 & 0 & \cos\left(\psi_d^*\right)\bar{u} - \sin\left(\psi_d^*\right)\bar{v} \\ 0 & 0 & 0 \end{bmatrix},$$

$$B_1(t) = \begin{bmatrix} \cos(\psi_d^*) & -\sin(\psi_d^*) & 0 \\ \sin(\psi_d^*) & \cos(\psi_d^*) & 0 \\ 0 & 0 & 1 \end{bmatrix}.$$

To increase the control quality of the kinematics loop, a PI feedback control law is designed as

$$\underbrace{\begin{bmatrix} \tilde{u} \\ \tilde{v} \\ \tilde{r} \end{bmatrix}}_{:=\tilde{\upsilon}} = -K_{P1}\begin{bmatrix} e_x \\ e_y \\ e_\psi \end{bmatrix} - K_{I1}\begin{bmatrix} \int e_x dt \\ \int e_y dt \\ \int e_\psi dt \end{bmatrix} \tag{20}$$

Define the augmented the kinematics loop error as

$$\begin{aligned} E_{\Omega 1} &= \begin{bmatrix} \int E_1 dt & E_1 \end{bmatrix}^T \\ &= \begin{bmatrix} \int e_x dt & \int e_y dt & \int e_\psi dt & e_x & e_y & e_\psi \end{bmatrix}^T \end{aligned} \tag{21}$$

From (20) and (21), the tracking error can be rewritten as

$$\begin{aligned} \dot{E}_{\Omega 1} &= A_{1c}E_{\Omega 1} \\ &= \begin{bmatrix} 0_3 & I_3 \\ -B_1K_{I1} & A_1 - B_1K_{P1} \end{bmatrix} E_{\Omega 1} \end{aligned} \tag{22}$$

where 0_3 and I_3 represent 3×3 zero matrix and identity matrix, respectively.

The desired tracking error dynamics can be constructed as

$$A_{1c} = \begin{bmatrix} 0_3 & I_3 \\ H_{11}(t) & H_{12}(t) \end{bmatrix} \tag{23}$$

where $H_{11}(t) = diag(-a_{111}, -a_{121}, -a_{131})$, $H_{12}(t) = diag(-a_{112}, -a_{122}, -a_{132})$, in which $a_{1j1} > 0$, $a_{1j2} > 0$ $(j = 1, 2, 3)$ can be gained from the second-order LTV differential equation [17], [18]. If the PD-eigenvalues satisfy $\rho_1(t) = -\left(\xi_{1j} \pm \sqrt{1-\xi_{1j}^2}\right)\omega_{1j}(t)$, which can be chosen as

$$\begin{aligned} a_{1j1} &= \omega_{1j}^2(t) \\ a_{1j2} &= \xi_{1j}\omega_{1j}(t) - \frac{\dot{\omega}_{1j}(t)}{\omega_{1j}(t)} \end{aligned} \tag{24}$$

where ξ_{1j} represents constant damping, $\omega_{1j}(t)$ represents the closed-loop bandwidth. At this point, we can obtain

$$\begin{aligned} K_{I1} &= -B_1^{-1}(t)H_{11}(t) \\ K_{P1} &= B_1^{-1}(t)(A_1(t) - H_{12}(t)) \end{aligned} \tag{25}$$

Therefore, the control command of kinematic loop can be expressed as

$$\upsilon^* = \bar{\upsilon} + \tilde{\upsilon} \tag{26}$$

2) KINETIC CONTROL LOOP

In this subsection, the main task is to design a control law to track the control command of kinematics loop. When unmodeled dynamics and time-varying external disturbances are not considered, the pseudo inverse of (5) can be written as

$$\bar{\tau} = G_1(\upsilon^*)^{-1}(\dot{\upsilon}^* - F_1(\upsilon^*)) \tag{27}$$

where $\bar{\tau}$ denotes nominal kinetic controller, $\dot{\upsilon}^*$ is obtained by the υ^* through pseudo-differentiator $G_s(s) = \frac{4s}{s+4}$.

For the kinetic loop tracking error $E_2 = \begin{bmatrix} e_u & e_v & e_r \end{bmatrix}^T$, from (9), we have

$$\begin{bmatrix} \dot{e}_u \\ \dot{e}_v \\ \dot{e}_r \end{bmatrix} = A_2(t)\begin{bmatrix} e_u \\ e_v \\ e_r \end{bmatrix} + B_2(t)\underbrace{\begin{bmatrix} \tilde{\tau}_u \\ \tilde{\tau}_v \\ \tilde{\tau}_r \end{bmatrix}}_{:=\tilde{\tau}} \tag{28}$$

where

$$A_2(t) = \begin{bmatrix} -\frac{d_{11}}{m_{11}} & \frac{m_{22}r^*}{m_{11}} & \frac{m_{22}v^*}{m_{11}} \\ -\frac{m_{11}r^*}{m_{22}} & -\frac{d_{22}}{m_{22}} & -\frac{m_{11}u^* + d_{23}}{m_{22}} \\ \frac{m_{11} - m_{22}}{m_{33}}v^* & \alpha_{11} & -\frac{d_{33}}{m_{33}} \end{bmatrix},$$

with $\alpha_{11} = \frac{(m_{11}u^* - m_{22}u^* - d_{32})}{m_{33}}$, $B_2(t) = diag\left(\frac{1}{m_{11}}, \frac{1}{m_{22}}, \frac{1}{m_{33}}\right)$.

Similarly, the PI control law is designed as

$$\underbrace{\begin{bmatrix} \tilde{\tau}_u \\ \tilde{\tau}_v \\ \tilde{\tau}_r \end{bmatrix}}_{:=\tilde{\tau}} = -K_{P2}\begin{bmatrix} e_u \\ e_v \\ e_r \end{bmatrix} - K_{I2}\begin{bmatrix} \int e_u dt \\ \int e_v dt \\ \int e_r dt \end{bmatrix} \tag{29}$$

Define the augmented kinetic loop error as

$$\begin{aligned} E_{\Omega 2} &= \begin{bmatrix} \int E_2 dt & E_2 \end{bmatrix}^T \\ &= \begin{bmatrix} \int e_u dt & \int e_v dt & \int e_r dt & e_u & e_v & e_r \end{bmatrix}^T \end{aligned} \tag{30}$$

Combining (29) and (30), the differential of the kinetic loop error can be summed up as

$$\begin{aligned} \dot{E}_{\Omega 2} &= A_{2c}E_{\Omega 2} \\ &= \begin{bmatrix} 0_3 & I_3 \\ -B_2K_{I2} & A_2 - B_2K_{P2} \end{bmatrix} E_{\Omega 2} \end{aligned} \tag{31}$$

The desired A_{2c} can be selected as

$$A_{1c} = \begin{bmatrix} 0_3 & I_3 \\ H_{21}(t) & H_{22}(t) \end{bmatrix} \tag{32}$$

where $H_{21}(t) = diag(-a_{211}, -a_{221}, -a_{231})$, $H_{22}(t) = diag(-a_{212}, -a_{222}, -a_{232})$. Similarly, a_{2j1} and a_{2j2} $(j = 1, 2, 3)$ still meet $\rho_2(t) = -\left(\xi_{2j} \pm \sqrt{1-\xi_{2j}^2}\right)\omega_{2j}(t)$, we obtain

$$\begin{aligned} a_{2j1} &= \omega_{2j}^2(t) \\ a_{2j2} &= \xi_{2j}\omega_{2j}(t) - \frac{\dot{\omega}_{2j}(t)}{\omega_{2j}(t)} \end{aligned} \tag{33}$$

Then we have

$$\begin{aligned} K_{I2} &= -B_2^{-1}(t)H_{21}(t) \\ K_{P2} &= B_2^{-1}(t)(A_2(t) - H_{22}(t)) \end{aligned} \tag{34}$$

Hence, the time-varying linear feedback law τ_k of the kinetic loop is

$$\tau_k = \bar{\tau} - K_{P2}E_2 - K_{I2}\int_0^t E_2 d\iota \tag{35}$$

3) ADAPTIVE COMPENSATION CONTROLLER

In this subsection, a reduced-order ESO is constructed to estimate and compensate for unknown time-varying disturbances. From [24], the novel reduced-order ESO is proposed as (36)

$$\begin{cases} \dot{\rho}_1 = -\beta_1 \rho_1 - \beta_1^2 \upsilon - \beta_1 \phi \\ \hat{d} = \rho_1 + \beta_1 \upsilon \end{cases} \tag{36}$$

where $\phi = F_1(\upsilon) + G_1(\upsilon)\tau + G_3(\upsilon)\Xi(\upsilon)$, $\hat{d}$ denotes the estimate of d, and its estimation error is $\tilde{d} = d - \hat{d}$. In addition, ρ_1 and $\beta_1 > 0$ are the observe auxiliary state and the observer gain, respectively. Define $\nu_d = \hat{d}$, then the output of disturbance compensation is $u_0 = G_0(\upsilon)\nu_d$.

Due to the augmented kinetic loop error, (3) can be written as follows

$$\dot{X}_2 = F_{11}(X_2) + G_{11}(X_2)\tau + G_{33}(X_2)\Xi(\upsilon) + G_{22}(X_2)d(t) \tag{37}$$

where $X_2 = \left[\int \upsilon dt \;\; \upsilon\right]^T$, $F_{11}(X_2) = \left[\upsilon \;\; F_1(\upsilon)\right]^T$, $G_{11}(X_2) = \left[0_3 \;\; G_1(\upsilon)\right]^T$, $G_{22}(X_2) = \left[0_3 \;\; G_2(\upsilon)\right]^T$, $G_{33}(X_2) = \left[0_3 \;\; G_3(\upsilon)\right]^T$. From (4), nonlinear matrix $G_0(\upsilon)$, $G_4(\upsilon)$ and $G_5(\upsilon)$ also meet the following conditions: $G_{11}(\upsilon)G_0(\upsilon) = G_{22}(\upsilon)$, $G_{11}(\upsilon)G_4(\upsilon) = G_{33}(\upsilon)$, $G_{22}(\upsilon)G_5(\upsilon) = G_{33}(\upsilon)$.

To improve the stability of the system, neural network MLP is hired to eliminate the effect of unmodeled dynamics. Define $\Psi_1 = E_{\Omega 2}^T P_2(t)$, $\Psi_2 = E_{\Omega 2}^T P_2(t) G_{22}(X_2)$, $\Psi_3 = E_{\Omega 2}^T P_2(t) G_{33}(X_2)$, where $P_2(t)$ is a positive symmetric matrix. The compensation controller u_n is selected as follows

$$u_n = G_4(\upsilon)\nu_n \tag{38}$$

where $\nu_n = \frac{1}{2}\Psi_3^T \hat{\Phi} \Theta^T \Theta$, in order to avoid parameter drift, the adaptive law with "κ-correction" is designed as

$$\dot{\hat{\Phi}} = \frac{\Gamma_1}{2}\Psi_3 \Psi_3^T \Theta^T \Theta - \kappa \Gamma_1 \hat{\Phi} \tag{39}$$

where Γ_1 and κ are two design parameters.

Meanwhile, to further improve the performance of the control system, the adaptive robust control term is designed to eliminate the estimation errors of neural network and reduced-order ESO.

Then robust control term controller u_r is selected as

$$u_r = G_0(\upsilon)\nu_r \tag{40}$$

where $\nu_r = \hat{\omega}\,\mathrm{sgn}(\Psi_2)$, in which the adaptive law is proposed as

$$\dot{\hat{\omega}} = \Gamma_2 \Psi_2^T - \Gamma_2 \gamma \hat{\omega} \tag{41}$$

where Γ_2 and γ are two design parameters.

From the section D, an auxiliary system is constructed to solve input saturation, which is rewritten as

$$\dot{\zeta} = \begin{cases} -K_\zeta \zeta - \dfrac{\sum_{i=1}^{3} |E_{\Omega 2i}\Delta\tau_i| + 0.5\Delta\tau^T\Delta\tau}{\|\zeta^2\|} \cdot \zeta & \\ +\Delta\tau, & \|\zeta\| > \sigma \\ 0_{3\times 1}, & \|\zeta\| < \sigma \end{cases} \tag{42}$$

The control law τ_o can be modified by

$$\tau_o = \tau_k + u_s - u_n - u_0 - u_r \tag{43}$$

where $u_s = K_s\zeta$, $K_s = K_s^T \in R^{3\times 3}$ is a positive design matrix, and we define $\Psi_4 = P_2(t) G_{11}(X_2) K_s$.

Hence, the total control law is designed as

$$\tau = \begin{cases} \tau_{\max}, & if\ \tau_o > \tau_{\max} \\ \tau_o, & if\ \tau_{\min} < \tau_o < \tau_{\max} \\ \tau_{\min}, & if\ \tau_o < \tau_{\min} \end{cases} \tag{44}$$

IV. STABILITY ANALYSIS

By the above control law, the differential of $E_{\Omega 1}$ and $E_{\Omega 2}$ can be rewritten as

$$\begin{aligned} \dot{E}_{\Omega 1} &= f_{11}(t, E_{\Omega 1}) \\ &= A_{1c}(t)E_{\Omega 1} + o_1(\bullet) \\ \dot{E}_{\Omega 2} &= f_{22}(t, E_{\Omega 2}) + G_{33}(X_2)(\theta F_1(\upsilon) - \nu_n) \\ &\quad + G_{22}(X_2)(d - \nu_d - \nu_r) + G_{11}(X_2)K_s\zeta \\ &= A_{2c}(t)E_{\Omega 2} + o_2(\bullet) + G_{33}(X_2)(\theta F_1(\upsilon) - \nu_n) \\ &\quad + G_{22}(X_2)(d - \nu_d - \nu_r) + G_{11}(X_2)K_s \end{aligned} \tag{45}$$

where $o_1(\bullet)$ and $o_2(\bullet)$ denote the high order term of the Taylor expansion, From [23], $o_1(\bullet)$ and $o_2(\bullet)$ satisfy $\|o_1(\bullet)\| \leq \ell_1\|E_{\Omega 1}\|^2, \forall \|E_{\Omega 1}\| < \alpha_1$ and $\|o_2(\bullet)\| \leq \ell_2\|E_{\Omega 2}\|^2, \forall \|E_{\Omega 2}\| < \alpha_2$, respectively. ℓ_1 and ℓ_2 are normal numbers.

Theorem 1 [33]: A_{mc} $(m = 1, 2)$ satisfies the following Lyapunov function candidate

$$A_{mc}^T(t)P_m(t) + P_m(t)A_{mc}(t) + \dot{P}_m(t) + Q_m(t) = 0 \tag{46}$$

where $P_m(t)$ is a positive symmetric matrix, $Q_m(t)$ is a continuous, bounded, positive definite, symmetric matrix. $P_m(t)$ and $Q_m(t)$ satisfy the following property: $0 < c_{1m}I \leq P_m(t) \leq c_{2m}I, \forall t \geqslant t_0$, $c_{1m} > 0$ and $c_{2m} > 0$; $0 < c_{3m}I \leq Q_m(t) \leq c_{4m}I, \forall t \geqslant t_0$, $c_{3m} > 0$ and $c_{4m} > 0$.

Theorem 2: Consider kinematics and kinetic dynamics equation presented as (1) and (2) under the control law (44), together with the reduced-order ESO (36), the adaptive laws (39) and (41). If the selected parameters satisfy the following conditions: 1) when $\|\zeta\| > \sigma$, we choose $c_{22} > 1$, $c_{31} > 2\ell_1\alpha_1 c_{21}$, $c_{32} > 2\ell_2\alpha_2 c_{22} + 1$; 2) when $\|\zeta\| < \sigma$, $c_{31} > 2\ell_1\alpha_1 c_{21}$, $c_{32} > 2\ell_2\alpha_2 c_{22} + 1$. The error signals of the whole system are uniformly ultimately bounded (UUB), and the tracking errors can be driven into a small neighborhood of origin.

Proof of Theorem 2: The Lyapunov function is constructed as following

$$V = \frac{1}{2}\left(E_{\Omega 1}^T P_1(t) E_{\Omega 1}\right) + \frac{1}{2}\left(E_{\Omega 2}^T P_2(t) E_{\Omega 2}\right) + \frac{1}{2}\Gamma_1^{-1}\tilde{\Phi}^2 + \frac{1}{2}\Gamma_2^{-1}\tilde{\omega}^T\tilde{\omega} + \frac{1}{2}\tilde{d}^T\tilde{d} + \frac{1}{2}\zeta^T\zeta \tag{47}$$

Differentiating (47) and substituting (45) into (47) yields

$$\begin{aligned}\dot{V} &= \frac{1}{2}E_{\Omega 1}^T\left(A_{1c}^T(t)P_1(t) + \dot{P}_1(t) + P_1(t)A_{1c}(t)\right)E_{\Omega 1} \\ &\quad + \frac{1}{2}E_{\Omega 2}^T\left(A_{2c}^T(t)P_2(t) + \dot{P}_2(t) + P_2(t)A_{2c}(t)\right)E_{\Omega 2} \\ &\quad + \Psi_3\left(W^T\Theta + \varepsilon - \frac{1}{2}\Psi_3^T\hat{\Phi}\Theta^T\Theta\right) + E_{\Omega 1}^T P_1(t)o_1(\bullet) \\ &\quad + \Psi_1(o_2(\bullet) + \Delta\tau) + E_{\Omega 2}^T\Psi_4\zeta + \Psi_2(d - \nu_d - \nu_r) \\ &\quad + \Gamma_1^{-1}\tilde{\Phi}\dot{\tilde{\Phi}} + \Gamma_2^{-1}\tilde{\omega}^T\dot{\tilde{\omega}} + \tilde{d}^T\dot{\tilde{d}} + \zeta^T\dot{\zeta}\end{aligned} \tag{48}$$

With the Theorem 1, $\dot{V}$ yields

$$\begin{aligned}\dot{V} &= -\frac{1}{2}E_{\Omega 1}^T Q_1(t)E_{\Omega 1} - \frac{1}{2}E_{\Omega 2}^T Q_2(t)E_{\Omega 2} \\ &\quad + \Psi_3\left(W^T\Theta - \frac{1}{2}\Psi_3^T\hat{\Phi}\Theta^T\Theta\right) + E_{\Omega 1}^T P_1(t)o_1(\bullet) \\ &\quad + \Psi_1(o_2(\bullet) + \Delta\tau) + E_{\Omega 2}^T\Psi_4\zeta \\ &\quad + \Psi_2\left(G_5(\upsilon)\varepsilon + \tilde{d} - \hat{\omega}\,\mathrm{sgn}(\Psi_2)\right) \\ &\quad + \Gamma_1^{-1}\tilde{\Phi}\dot{\tilde{\Phi}} + \Gamma_2^{-1}\tilde{\omega}\dot{\tilde{\omega}} + \tilde{d}^T\dot{\tilde{d}} + \zeta^T\dot{\zeta} \\ &\leq -\frac{1}{2}E_{\Omega 1}^T Q_1(t)E_{\Omega 1} - \frac{1}{2}E_{\Omega 2}^T Q_2(t)E_{\Omega 2} \\ &\quad + \tilde{\Phi}\left(-\frac{1}{2}\Psi_3\Psi_3^T\Theta^T\Theta + \Gamma_2^{-1}\dot{\tilde{\Phi}}\right) + \frac{1}{2} \\ &\quad + E_{\Omega 1}^T P_1(t)o_1(\bullet) + \Psi_1(o_2(\bullet) + \Delta\tau) + E_{\Omega 2}^T\Psi_4\zeta \\ &\quad + \Psi_2\left(G_5(\upsilon)\varepsilon + \tilde{d} - \hat{\omega}\,\mathrm{sgn}(\Psi_2)\right) \\ &\quad + \Gamma_2^{-1}\tilde{\omega}^T\dot{\tilde{\omega}} + \tilde{d}^T\dot{\tilde{d}} + \zeta^T\dot{\zeta}\end{aligned} \tag{49}$$

If $\left\|G_5(\upsilon)\varepsilon + \tilde{d}\right\| \leq \omega$, we have

$$\begin{aligned}\dot{V} &\leq -\frac{1}{2}E_{\Omega 1}^T Q_1(t)E_{\Omega 1} - \frac{1}{2}E_{\Omega 2}^T Q_2(t)E_{\Omega 2} \\ &\quad + \tilde{\Phi}\left(-\frac{1}{2}\Psi_3\Psi_3^T\Theta^T\Theta + \Gamma_2^{-1}\dot{\tilde{\Phi}}\right) + \frac{1}{2} \\ &\quad + E_{\Omega 1}^T P_1(t)o_1(\bullet) + \Psi_1(o_2(\bullet) + \Delta\tau) + E_{\Omega 2}^T\Psi_4\zeta \\ &\quad - \|\Psi_2\|\tilde{\omega} + \Gamma_2^{-1}\tilde{\omega}^T\dot{\tilde{\omega}} + \tilde{d}^T\dot{\tilde{d}} + \zeta^T\dot{\zeta}\end{aligned} \tag{50}$$

Submitting the adaptive laws (39) and (41), reduced-order ESO (36), we obtain

$$\begin{aligned}\dot{V} &\leq -\frac{1}{2}E_{\Omega 1}^T Q_1(t)E_{\Omega 1} - \frac{1}{2}E_{\Omega 2}^T Q_2(t)E_{\Omega 2} - \kappa\tilde{\Phi}\hat{\Phi} \\ &\quad + \frac{1}{2} + E_{\Omega 1}^T P_1(t)o_1(\bullet) + \Psi_1(o_2(\bullet) + \Delta\tau) \\ &\quad + E_{\Omega 2}^T\Psi_4\zeta - \gamma\tilde{\omega}^T\hat{\omega} - \frac{\beta_1}{2}\left\|\tilde{d}\right\|^2 + \zeta^T\dot{\zeta}\end{aligned} \tag{51}$$

From Young's inequality, we have $\tilde{\Phi}\hat{\Phi} \geqslant \frac{1}{2}\left(\tilde{\Phi}^2 - \Phi^2\right)$ and $\tilde{\omega}^T\hat{\omega} \geqslant \frac{1}{2}\left(\|\tilde{\omega}\|^2 - \|\omega\|^2\right)$. According to the above analysis, (51) can be written as

$$\begin{aligned}\dot{V} &\leq -\frac{1}{2}E_{\Omega 1}^T Q_1(t)E_{\Omega 1} - \frac{1}{2}E_{\Omega 2}^T Q_2(t)E_{\Omega 2} - \frac{\kappa}{2}\tilde{\Phi}^2 \\ &\quad - \frac{\gamma}{2}\|\tilde{\omega}\|^2 - \frac{\beta_1}{2}\left\|\tilde{d}\right\|^2 + E_{\Omega 1}^T P_1(t)o_1(\bullet) \\ &\quad + \Psi_1(o_2(\bullet) + \Delta\tau) + \frac{1}{2}\left\|E_{\Omega 2}^T\right\|^2 + \frac{1}{2}\zeta^T\Psi_4^T\Psi_4\zeta \\ &\quad + \frac{\kappa}{2}\Phi^2 + \frac{\gamma}{2}\|\omega\|^2 + \frac{1}{2} + \zeta^T\dot{\zeta}\end{aligned} \tag{52}$$

(1) when $\|\zeta\| > \sigma$, from (43) and Young's inequality, we have

$$\begin{aligned}\zeta^T\dot{\zeta} &= -\zeta^T K_\zeta\zeta - \sum_{i=1}^{3}|E_{2i}\Delta\tau_i| \\ &\quad - \frac{1}{2}\Delta\tau^T\Delta\tau + \zeta^T\Delta\tau \\ &\leq -\zeta^T K_\zeta\zeta - \sum_{i=1}^{3}|E_{2i}\Delta\tau_i| + \frac{1}{2}\zeta^T\zeta\end{aligned} \tag{53}$$

Substituting (53) into (52) yields

$$\begin{aligned}\dot{V} &\leq -\frac{1}{2}E_{\Omega 1}^T Q_1(t)E_{\Omega 1} - \frac{1}{2}E_{\Omega 2}^T Q_2(t)E_{\Omega 2} - \frac{\kappa}{2}\tilde{\Phi}^2 \\ &\quad - \frac{\gamma}{2}\|\tilde{\omega}\|^2 - \frac{\beta_1}{2}\left\|\tilde{d}\right\|^2 + E_{\Omega 1}^T P_1(t)o_1(\bullet) \\ &\quad + \Psi_1(o_2(\bullet) + \Delta\tau) + \frac{1}{2}\left\|E_{\Omega 2}^T\right\|^2 + \frac{1}{2}\zeta^T\Psi_4^T\Psi_4\zeta + \frac{\kappa}{2}\Phi^2 \\ &\quad + \frac{\gamma}{2}\|\omega\|^2 + \frac{1}{2} - \zeta^T K_\zeta\zeta - \sum_{i=1}^{3}|E_{2i}\Delta\tau_i| + \frac{1}{2}\zeta^T\zeta \\ &\leq -\frac{1}{2}(c_{31} - 2\ell_1\alpha_1 c_{21})\|E_{\Omega 1}\|^2 \\ &\quad - \frac{1}{2}(c_{32} - 2\ell_2\alpha_2 c_{22} - 1)\|E_{\Omega 2}\|^2 - \frac{\kappa}{2}\tilde{\Phi}^2 - \frac{\gamma}{2}\|\tilde{\omega}\|^2 \\ &\quad - \frac{\beta_1}{2}\left\|\tilde{d}\right\|^2 - \left[\chi_{\min}\left(K_\zeta - \frac{1}{2}\Psi_4^T\Psi_4\right) - \frac{1}{2}\right]\zeta^T\zeta \\ &\quad + (c_{22} - 1)\sum_{i=1}^{3}|E_{2i}\Delta\tau_i| + \frac{\kappa}{2}\Phi^2 + \frac{\gamma}{2}\|\omega\|^2 + \frac{1}{2}\end{aligned} \tag{54}$$

Set $\lambda_1 = \frac{1}{2}(c_{31} - 2\ell_1\alpha_1 c_{21}) > 0$, $\lambda_2 = \frac{1}{2}(c_{32} - 2\ell_2\alpha_2 c_{22} - 1)$, $\lambda_3 = \frac{\kappa}{2}$, $\lambda_4 = \frac{\gamma}{2}$, $\lambda_5 = \frac{\beta_1}{2}$, $\lambda_6 = \chi_{\min}\left(K_\zeta - \frac{1}{2}\Psi_4^T\Psi_4\right) - \frac{1}{2} > 0$, $\Lambda_1 = (c_{22} - 1)\sum_{i=1}^{3}|E_{2i}\Delta\tau_i| + \frac{\kappa}{2}\Phi^2 + \frac{\gamma}{2}\|\omega\|^2 + \frac{1}{2}$, (54) becomes

$$\begin{aligned}\dot{V} &\leq -\lambda_1\|E_{\Omega 1}\|^2 - \lambda_2\|E_{\Omega 2}\|^2 - \lambda_3\tilde{\Phi}^2 - \lambda_4\|\tilde{\omega}\|^2 \\ &\quad - \lambda_5\left\|\tilde{d}\right\|^2 - \lambda_6\zeta^T\zeta + \Lambda_1\end{aligned} \tag{55}$$

Define $\lambda_{11} = \min\{\lambda_1, \lambda_2, \lambda_3, \lambda_4, \lambda_5, \lambda_6\}$, then it follows form (55) that

$$\dot{V} \leq -2\lambda_{11}V + \Lambda_1 \tag{56}$$

Solving inequality (56) gives

$$\dot{V} \leq \left(V(0) - \frac{\Lambda_1}{2\lambda_{11}}\right) e^{-2\lambda_{11}t} + \frac{\Lambda_1}{2\lambda_{11}} \leq V(0)\, e^{-2\lambda_{11}t} + \frac{\Lambda_1}{2\lambda_{11}}, \forall t > 0 \tag{57}$$

(2) when $\|\zeta\| < \sigma$, from (43) and Young's inequality, we have

$$\zeta^T \dot{\zeta} = 0 \tag{58}$$

$$\frac{1}{2}\zeta^T \Psi_4^T \Psi_4 \zeta = -\frac{1}{2}\zeta^T \Psi_4^T \Psi_4 \zeta + \zeta^T \Psi_4^T \Psi_4 \zeta \leq -\frac{1}{2}\zeta^T \Psi_4^T \Psi_4 \zeta + \sigma^2 \left\|\Psi_4^T \Psi_4\right\| \tag{59}$$

$$\Psi_1 \Delta\tau \leq \frac{1}{2}\Psi_1 \Psi_1^T + \frac{1}{2}\|\Delta\tau\|^2 \tag{60}$$

Substituting (58), (59) and (60) into (52) yields

$$\begin{aligned}\dot{V} \leq& -\frac{1}{2}E_{\Omega 1}^T Q_1(t) E_{\Omega 1} - \frac{1}{2}E_{\Omega 2}^T Q_2(t) E_{\Omega 2} - \frac{\kappa}{2}\tilde{\Phi}^2 \\ &- \frac{\gamma}{2}\|\tilde{\omega}\|^2 - \frac{\beta_1}{2}\left\|\tilde{d}\right\|^2 + E_{\Omega 1}^T P_1(t)\, o_1(\bullet) + \Psi_1 o_2(\bullet) \\ &+ \frac{1}{2}\left\|E_{\Omega 2}^T\right\|^2 - \frac{1}{2}\zeta^T \Psi_4^T \Psi_4 \zeta + \sigma^2 \left\|\Psi_4^T \Psi_4\right\| \\ &+ \frac{1}{2}\Psi_1 \Psi_1^T + \frac{1}{2}\|\Delta\tau\|^2 + \frac{\kappa}{2}\Phi^2 + \frac{\gamma}{2}\|\omega\|^2 + \frac{1}{2} \\ \leq& -\frac{1}{2}(c_{31} - 2\ell_1\alpha_1 c_{21})\|E_{\Omega 1}\|^2 \\ &- \frac{1}{2}(c_{32} - 2\ell_2\alpha_2 c_{22} - 1)\|E_{\Omega 2}\|^2 - \frac{\kappa}{2}\tilde{\Phi}^2 \\ &- \frac{\gamma}{2}\|\tilde{\omega}\|^2 - \frac{\beta_1}{2}\left\|\tilde{d}\right\|^2 - \frac{1}{2}\chi_{\min}\left(\Psi_4^T \Psi_4\right)\zeta^T\zeta \\ &+ \frac{1}{2}\left\|\Psi_1 \Psi_1^T\right\| + \frac{1}{2}\|\Delta\tau\|^2 + \sigma^2\left\|\Psi_4^T \Psi_4\right\| \\ &+ \frac{\kappa}{2}\Phi^2 + \frac{\gamma}{2}\|\omega\|^2 + \frac{1}{2}\end{aligned} \tag{61}$$

Set $\lambda_7 = \frac{1}{2}\chi_{\min}\left(\Psi_4^T\Psi_4\right)$, $\Lambda_2 = \frac{1}{2}\left\|\Psi_1\Psi_1^T\right\| + \frac{1}{2}\|\Delta\tau\|^2 + \sigma^2\left\|\Psi_4^T\Psi_4\right\| + \frac{\kappa}{2}\Phi^2 + \frac{\gamma}{2}\|\omega\|^2 + \frac{1}{2}$, (61) becomes

$$\dot{V} \leq -\lambda_1\|E_{\Omega 1}\|^2 - \lambda_2\|E_{\Omega 2}\|^2 - \lambda_3\tilde{\Phi}^2 - \lambda_4\|\tilde{\omega}\|^2 - \lambda_5\left\|\tilde{d}\right\|^2 - \lambda_7\zeta^T\zeta + \Lambda_2 \tag{62}$$

Define $\lambda_{22} = \min\{\lambda_1, \lambda_2, \lambda_3, \lambda_4, \lambda_5, \lambda_7\}$, then it follows form (62) that

$$\dot{V} \leq -2\lambda_{22}V + \Lambda_2 \tag{63}$$

Solving inequality (63) gives

$$\dot{V} \leq \left(V(0) - \frac{\Lambda_2}{2\lambda_{22}}\right) e^{-2\lambda_{22}t} + \frac{\Lambda_2}{2\lambda_{22}} \leq V(0)\, e^{-2\lambda_{22}t} + \frac{\Lambda_2}{2\lambda_{22}}, \quad \forall t > 0 \tag{64}$$

Through the above inference, it can be seen that V is eventually bounded by $\frac{\Lambda_1}{2\lambda_{11}}$ or $\frac{\Lambda_2}{2\lambda_{22}}$. Therefore, $\frac{\Lambda_1}{2\lambda_{11}}$ or $\frac{\Lambda_2}{2\lambda_{22}}$ can be made arbitrarily small with the appropriately chosen parameters, and the whole error signals are UUB.

V. NUMERICAL SIMULATIONS

A. CONTROL PARAMETERS ADJUSTMENT SUGGESTIONS

In order to adjust the trajectory tracking control parameters faster and more accurately, many adjustment strategies are given for control parameters: ξ_{1_j}, ω_{1j}, ξ_{2_j}, ω_{2j}, K_ζ, K_s, h_1, r_1, Γ_1, κ, β_1, Γ_2, γ. The purpose of properly adjusting the parameters is to improve the control performance of the system by reducing tracking error or reasonable tracking speed. However, it is difficult to reduce tracking error or reasonable tracking speed at the same time. Therefore, all parameters need to be considered as a whole to enhance the control performance of the system.

(1) For TLC control parameters, first, the feedback gains ξ_{1_j} and ξ_{2_j} should satisfy condition of the eigenvalue. Then the closed-loop bandwidth ω_{1j} and ω_{2j} should satisfy the surface vessels tracking requirement, and the kinetic loop bandwidth should be at least three times higher than the kinematic loop to satisfy the singular perturbation assumption. In addition, the closed-loop bandwidth should be as low as possible. This is because the lower bandwidth can reduce power consumption and noise in the control process.

(2) h_1 and r_1 are the control parameters of NTD. The size of acceleration factor r_1 determines the tracking speed of NTD. As r_1 becomes larger, the tracking speed is faster. The small sampling period h_1 can reduce noise. Therefore, the proper adjustment h_1 and r_1 can accurately track a given signal.

(3) Large values of adaptive gain Γ_1 and Γ_2 can improve the learning speed of neural network MLP and the ability of robust term to compensate error, respectively. Here, κ and γ of the selection are too small, which makes the value of Λ_1 and Λ_2 smaller. However, the value of Λ_1 and Λ_2 will directly affect the robustness of (39) and (41).

(4) β_1, K_ζ and K_s need to be adjusted within a range. If all are too large or too small, which will affect the performance of reduced-order ESO and auxiliary design system. Therefore, in the process of adjusting parameters, it needs to be optimized and adjusted together with ξ_{1_j}, ω_{1j}, ξ_{2_j}, ω_{2j}, h_1, r_1, Γ_1, κ, Γ_2, γ.

B. SIMULATION RESULTS AND COMPARISON

In order to demonstrate the effectiveness of the proposed scheme, we compare it with three control methods: backstepping with integrator control strategy [46], adaptive dynamic surface SMC [47] and PID control strategy. For this purpose, CyberShip II [48], [49] is taken as the control object. Relevant parameters of the dynamics for CyberShip II are described in the Table 1. In addition, the tuned controller parameters and initial parameters are listed in the Table 2.

In the simulation, the reference path:

$$\eta_d = \begin{bmatrix} x_d \\ y_d \\ \psi_d \end{bmatrix} = \begin{bmatrix} 2.5\sin(0.02t) \\ 2.5(1 - \cos(0.02t)) \\ 0.02t \end{bmatrix}.$$

TABLE 1. Parameters of the model ship.

Parameter	Value
m_{11}	25.8
m_{22}	33.8
m_{33}	2.76
c_{13}	-33.8v-1.0115r
c_{23}	25.8u
c_{31}	$-c_{13}$
c_{32}	$-c_{23}$
d_{11}	0.72
d_{22}	0.8896
d_{23}	7.25
d_{32}	0.0313
d_{33}	1.9

TABLE 2. Initial conditions and controller parameters.

	Parameter Value
Initial conditions for surface vehicle	$\eta(0) = [0.1m; 0.2m; 0.1rad]$, $\upsilon(0) = [0m/s; 0m/s; 0rad/s]$
backstepping with integrator method	$C_1 = diag(40, 40, 40)$, $C_2 = diag(150, 150, 150)$, $K = diag(5, 5, 5)$
adaptive SMC	$K_0 = diag(3, 3, 3)$, $K_1 = diag(0.8, 0.8, 0.8)$, $K_2 = diag(100, 100, 100)$, $\Gamma = diag(10, 10, 10)$
PID method	$K_p = diag(5000, 3500, 3500)$, $K_i = diag(200, 200, 200)$, $K_d = diag(1000, 600, 200)$
NTD	$h_1 = 0.02s$, $r_1 = 0.06rad/s^2$
the kinematics loop	$\xi_{1j} = 0.7\,(j = 1, 2, 3)$, $\omega_{1j} = 2.5$, $Q_1(t) = 0.5I_6$
the kinetic loop	$\xi_{2j} = 0.9\,(j = 1, 2, 3)$, $\omega_{2j} = 10$, $Q_2(t) = 0.9I_6$, $\Gamma_1 = 100$, $\kappa = 0.5$, $\beta_1 = 10$, $\Gamma_2 = 0.001$, $\gamma = 0.01$, $K_\zeta = diag(2, 2, 2)$, $K_s = diag(1, 1, 1)$, $\zeta = 0.1$, $\tau_{1\max} = 240N$, $\tau_{1\min} = -240N$, $\tau_{2\max} = 250N$, $\tau_{2\min} = -250N$, $\tau_{3\max} = 150\,(Nm)$, $\tau_{3\min} = -150\,(Nm)$

Finally, in order to show the results of comparison more clearly, ITAE index is hired to quantify the tracking error [50].

$$ITAE = \int_0^t t\,|\eta_d - \eta|\,dt \tag{65}$$

In order to demonstrate the effectiveness and robustness of the proposed scheme, without changing any control parameters, we consider the system in two cases. The first case is that a small uncertainty and disturbance are employed. The second case is that a large uncertainty and disturbance are considered.

Case 1: The unmodeled degree coefficient $\theta = diag(0.6, 0.6, 0.6)$, according to [6], the multiple disturbances are

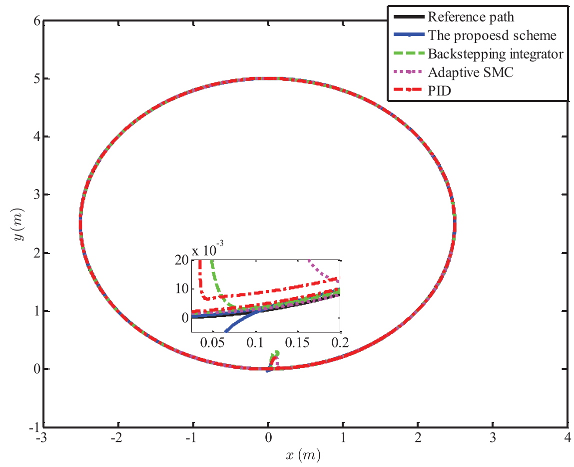

FIGURE 4. Tracking trajectory performance under case 1.

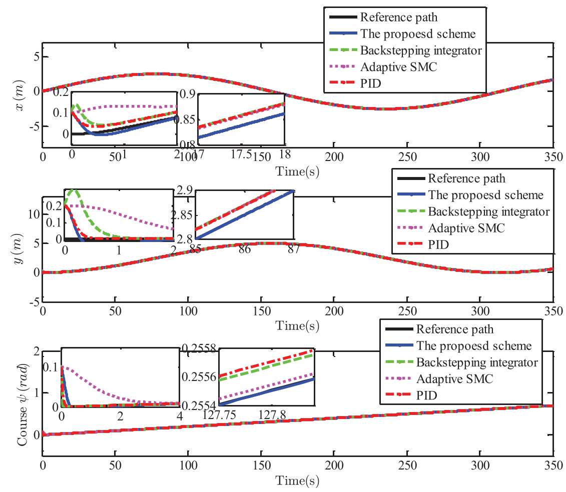

FIGURE 5. Tracking trajectory results under case 1.

given as

$$d(t) = \begin{bmatrix} 0.5 + 0.1\sin(0.2t) + 0.3\cos(0.1t)N \\ 0.5 + 0.2\sin(0.2t) + 0.2\cos(0.4t)N \\ 0.5 + 0.1\sin(0.1t) + 0.1\cos(0.2t)Nm \end{bmatrix} \tag{66}$$

The circular path simulation results are shown in Figs. 4-8. In addition, the ITAE index of the tracking error is reported in Table 3.

Fig. 4 demonstrates the comparison performance of tracking trajectory under a small unmodeled dynamics and unknown time-varying disturbances. From Fig. 4, it is obviously observed that all the four controllers provide very good tracking performance for the system. However, as the results shown in Fig. 4, the proposed scheme converges faster than that of backstepping with integrator, adaptive SMC and PID. In addition, the tracking trajectory results of the controllers are further shown in Fig. 5. We can see that the tracking results of the proposed scheme is the the best in the four control methods. Fig. 6 shows the control efforts of these four control strategies. It can be clearly observed that the

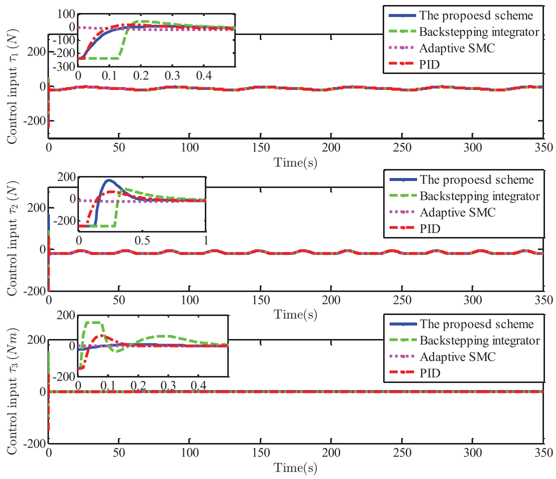

FIGURE 6. Control efforts of the controllers under case 1.

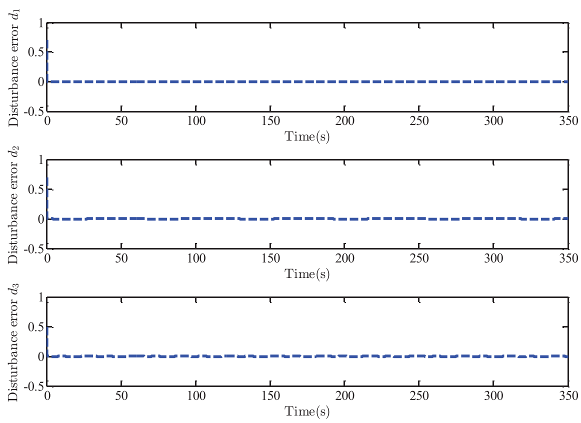

FIGURE 7. Disturbance estimation error under case 1.

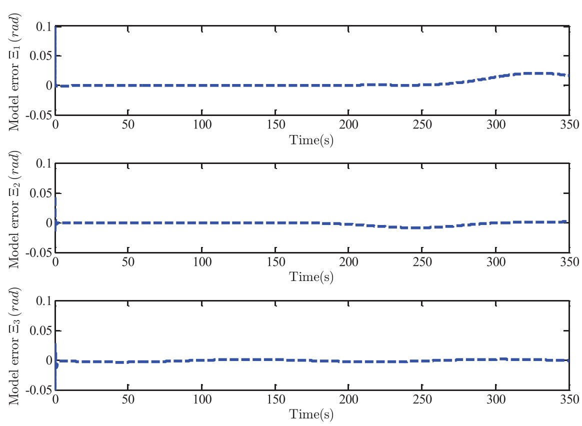

FIGURE 8. Unmodeled dynamics estimation error under case 1.

control inputs of backstepping with integrator controller and PID controller exceed the maximum value of the propulsion system. But only τ_2 of the proposed scheme has input saturation. This is because NTD and pseudo-differentiators are used in the proposed scheme, input saturation phenomenon is directly avoided within a certain range, and much

TABLE 3. ITAE index under case 1.

ITAE	Value
The proposed scheme	$\text{ITAE}_x = 2.991$
	$\text{ITAE}_y = 2.643$
	$\text{ITAE}_\psi = 0.102$
backstepping with integrator	$\text{ITAE}_x = 44.77$
	$\text{ITAE}_y = 53.32$
	$\text{ITAE}_\psi = 2.427$
Adaptive SMC	$\text{ITAE}_x = 44.6$
	$\text{ITAE}_y = 76.49$
	$\text{ITAE}_\psi = 4.369$
PID	$\text{ITAE}_x = 59.92$
	$\text{ITAE}_y = 81.02$
	$\text{ITAE}_\psi = 3.574$

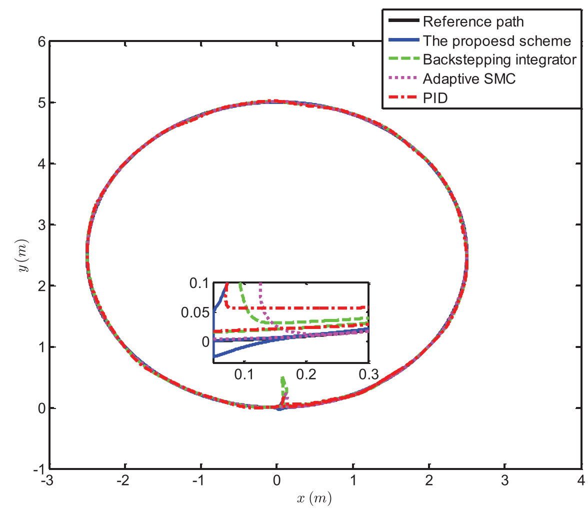

FIGURE 9. Tracking trajectory performance under case 2.

smaller forces are generated. Fig. 7 and 8 clearly demonstrate that disturbance estimation errors and unmodeled dynamics estimation errors are almost zero. From the ITAE value in Table 3, we can see that the error values of the four controllers are $[2.991, 2.643, 0.102]^T$, $[44.77, 53.32, 2.427]^T$, $[44.6, 76.49, 4.369]^T$ and $[59.92, 81.02, 3.574]^T$, respectively. The responses of the proposed scheme is better than the backstepping with integrator, adaptive SMC and PID, and it is only $[6.68\%, 4.96\%, 4.2\%]^T$ of backstepping with integrator, $[6.7\%, 3.46\%, 2.33\%]^T$ of adaptive SMC and $[4.99\%, 3.26\%, 2.85\%]^T$ of PID. Through the above analysis, we can conclude that the proposed scheme is the best among controllers in faster convergence speed, tracking performance and lower tracking error.

Case 2: The unmodeled degree coefficient $\theta = diag(6, 6, 6)$, the multiple disturbances are given as

$$d(t) = \begin{bmatrix} 10\,(0.5 + 0.1\sin(0.2t) + 0.3\cos(0.1t))\,N \\ 10\,(0.5 + 0.2\sin(0.2t) + 0.2\cos(0.4t))\,N \\ 10\,(0.5 + 0.1\sin(0.1t) + 0.1\cos(0.2t))\,Nm \end{bmatrix} \quad (67)$$

Simulation results are demonstrated in Figs. 9-13. Similarly, the ITAE index of the tracking error is reported in Table 4.

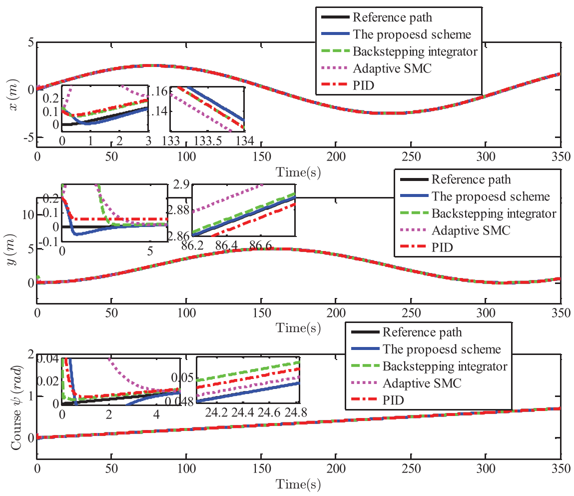

FIGURE 10. Tracking trajectory results under case 2.

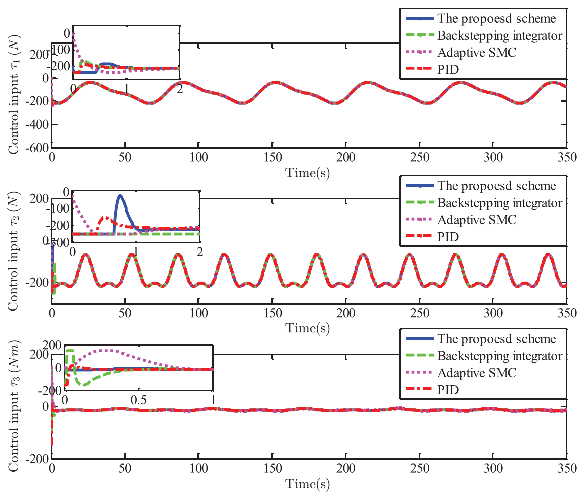

FIGURE 11. Control efforts of the controllers under case 2.

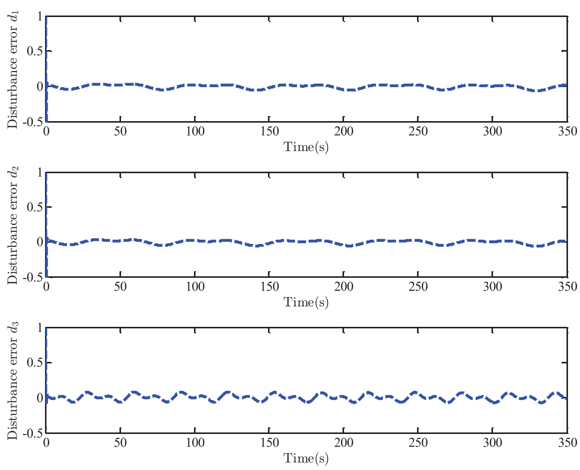

FIGURE 12. Disturbance estimation error under case 2.

The tracking performance and results of four control methods are demonstrated in Figs. 9-10. From Figs. 9-10, we can see that the backstepping with integrator, adaptive

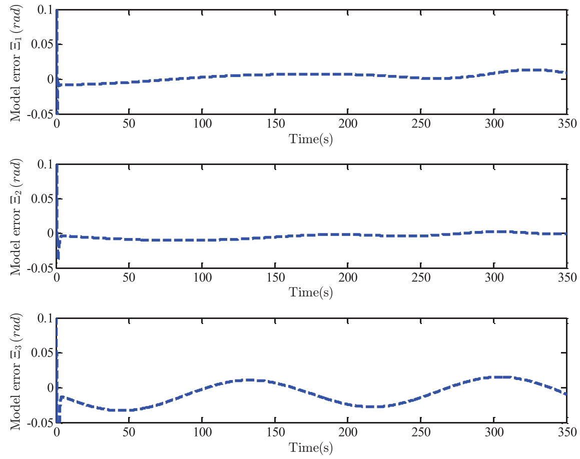

FIGURE 13. Unmodeled dynamics estimation error under case 2.

TABLE 4. ITAE Index under case 2.

ITAE	Value
The proposed scheme	$ITAE_x = 3.428$ $ITAE_y = 7.493$ $ITAE_\psi = 1.141$
backstepping with integrator	$ITAE_x = 451.4$ $ITAE_y = 533.6$ $ITAE_\psi = 24.62$
Adaptive SMC	$ITAE_x = 88.36$ $ITAE_y = 162$ $ITAE_\psi = 16.87$
PID	$ITAE_x = 600.4$ $ITAE_y = 812.6$ $ITAE_\psi = 34.93$

SMC and PID provide worst tracking response and precision in a large uncertainty and disturbance. On the other hand, as shown in Fig. 9, the proposed scheme converges faster and provides better tracking performance than the backstepping with integrator, adaptive SMC and PID. Fig. 11 depicts control efforts of four control methods. From Fig. 11, it is clearly noticed that the controllers have reached saturation at the beginning. Due to a large disturbance and control gain, the controllers produce initial values greater than the actuator output capability. Hence, it is necessary to take into account input saturation. Fig. 12 and 13 show that disturbance estimation errors and unmodeled dynamics estimation errors can still converge to zero quickly, and eventually maintains stable near zero. In addition, Table 4 shows the greatest advantage of the proposed scheme. From the ITAE value in Table 4, we can see that the error value of the proposed scheme is $[3.428, 7.493, 1.141]^T$, and it is only $[0.76\%, 1.40\%, 4.63\%]^T$ of backstepping with integrator, $[3.88\%, 4.63\%, 6.76\%]^T$ of adaptive SMC and $[0.57\%, 0.92\%, 3.27\%]^T$ of PID. Despite a large uncertainty and disturbance, the value of ITAE increased from $[2.991, 2.643, 0.102]^T$ to $[3.428, 7.493, 1.141]^T$, increasing by only $[0.437, 4.850, 1.039]^T$. Obviously, in terms of tracking error, the proposed scheme provides much lower tracking error and stronger robustness compared to the backstepping with integrator, adaptive SMC and PID. Therefore, based on the above analysis and results, when considering the performance of the controllers in all aspects of a control system such as tracking precision, convergence speed, control efforts and the robustness, the proposed scheme is the best among the compared four control strategies.

VI. CONCLUSION

In this paper, on the basis of considering the saturation of the actuator, a novel robust compound control scheme has been developed for tracking control of fully actuated surface vessels with unmodeled dynamics and unknown time-varying disturbances. The key to this article is that TLC technology is first applied to the design of trajectory tracking controller for surface vessel. Combining TLC technology, neural network, reduced-order ESO, NTD and auxiliary dynamic system, an adaptive trajectory tracking controller is design, which not only can eliminate the influence of the system uncertainties but also can improve tracking accuracy. More importantly, in contrast to traditional control algorithm, the proposed scheme has a strong robustness. All signals in the the whole system are guaranteed by Lyapunov stability theory. The proposed scheme has been tested in the simulated surface vessel and compared with other control methods. The results demonstrated the superior performance of the developed control strategy.

Many effective techniques including TLC, MLP and ESO, aims to handle a series of problems in trajectory tracking control rather than a specific unmodeled dynamics and time-varying external disturbances problems. Therefore, further work will also include problems of underactuated nonlinear uncertain system, the finite time trajectory tracking and their relationship.

ACKNOWLEDGMENT

The authors declare no conflict of interest.

REFERENCES

[1] B. Xiao, X. B. Yang, and X. Huo, "A novel disturbance estimation scheme for formation control of ocean surface vessels," *IEEE Trans. Ind. Electron.*, vol. 64, no. 6, pp. 4994–5003, Jun. 2017.

[2] S. L. Dai, M. Wang, and C. Wang, "Neural learning control of marine surface vessels with guaranteed transient tracking performance," *IEEE Trans. Ind. Electron.*, vol. 63, no. 3, pp. 1717–1727, Mar. 2016.

[3] G. B. Zhu and J. Du, "Global robust adaptive trajectory tracking control for surface ships under input saturation," *IEEE J. Ocean. Eng.*, to be published, doi: 10.1109/JOE.2018.2877895.

[4] M.-C. Fang, Y.-Z. Zhuo, and Z.-Y. Lee, "The application of the self-tuning neural network PID controller on the ship roll reduction in random waves," *Ocean Eng.*, vol. 37, no. 7, pp. 529–538, May 2010.

[5] J. M. Larrazabal and M. S. Peñas, "Intelligent rudder control of an unmanned surface vessel," *Expert Syst. Appl.*, vol. 55, pp. 106–117, Aug. 2016.

[6] D. D. Mu, G. F. Wang, and Y. S. Fan, "Tracking control of podded propulsion unmanned surface vehicle with unknown dynamics and disturbance under input saturation," *Int. J. Control Autom. Syst.*, vol. 16, no. 4, pp. 1905–1915, Aug. 2018.

[7] M. Abdelaal, M. Franzle, and A. Hahn, "Nonlinear model predictive control for trajectory tracking and collision avoidance of underactuated vessels with disturbances," *Ocean Eng.*, vol. 160, pp. 168–180, Jul. 2018.

[8] Z. Yin, W. He, C. Yang, and C. Sun, "Control design of a marine vessel system using reinforcement learning," *Neurocomputing*, vol. 311, pp. 353–362, Oct. 2018, doi: 10.1016/j.neucom.2018.05.061.

[9] Y. Zhang, S. Li, and X. Liu, "Adaptive near-optimal control of uncertain systems with application to underactuated surface vessels," *IEEE Trans Control Syst Technol.*, vol. 26, no. 4, pp. 1204–1218, Jul. 2018.

[10] K. Jiang, B. Niu, J. Li, P. Duan, and J. Wang, "Adaptive neural controller design scheme of nonlinear delayed systems with completely unknown nonlinearities and non-strict-feedback structure," *IEEE Access*, vol. 6, pp. 66418–66427, 2018, doi: 10.1109/ACCESS.2018.2877798.

[11] Y. Z. Qian, Y. C. Fang, and T. Yang, "An energy-based nonlinear coupling control for offshore ship-mounted cranes," *Int. J. Autom. Comput.*, vol. 15, no. 5, pp. 570–581, Oct. 2018.

[12] B. Niu, D. Wang, N. D. Alotaibi, and F. E. Alsaadi, "Adaptive neural state-feedback tracking control of stochastic nonlinear switched systems: An average dwell-time method," *IEEE Trans. Neural Netw. Learn. Syst.*, to be published, doi: 10.1109/TNNLS.2018.2860944.

[13] B. Niu, H. Li, Z. Zhang, J. Li, T. Hayat, and F. Alsaadi, "Adaptive neural-network-based dynamic surface control for stochastic interconnected nonlinear nonstrict-feedback systems with dead zone," *IEEE Trans. Syst., Man, Cybern. Syst.*, to be published, doi: 10.1109/TSMC.2018.2866519.

[14] Y. Qian, Y. Fang, and B. Lu, "Adaptive robust tracking control for an offshore ship-mounted crane subject to unmatched sea wave disturbances," *Mech. Syst. Signal Process.*, vol. 114, no. 5, pp. 556–570, Jan. 2018.

[15] J. Yao, Z. Jiao, and D. Ma, "Adaptive robust control of DC motors with extended state observer," *IEEE Trans. Ind. Electron.*, vol. 61, no. 7, pp. 3630–3637, Jul. 2014.

[16] M. C. Mickle and J. J. Zhu, "Skid to turn control of the APKWS missile using trajectory linearization technique," in *Proc. Amer. Control Conf.*, vol. 5, pp. 3346–3351, Jul. 2001.

[17] J. Zhu, B. Banker, and C. Hall, "X-33 ascent flight control design by trajectory linearization—A singular perturbation approach," in *Proc. AIAA. Guid., Navigat. Control. Conf.*, 2006, p. 4159.

[18] B. Zhu and W. Huo, "Adaptive trajectory linearization control for a model-scaled helicopter with uncertain inertial parameters," in *Proc. Chin. Control. Conf. (CCC)*, 2012, pp. 4389–4395.

[19] T. M. Adami and J. J. Zhu, "6 DOF flight control of fixed-wing aircraft by trajectory linearization," in *Proc. Amer. Control. Conf.*, 2011, pp. 1610–1617.

[20] Z. Sun, G. Zhang, and L. Qiao, "Robust adaptive trajectory tracking control of underactuated surface vessel in fields of marine practice," *J. Marine Sci. Technol.*, vol. 23, no. 4, pp. 950–957, Dec. 2018.

[21] Y. Pan, C. Yang, L. Pan, and H. Yu, "Integral sliding mode control: Performance, modification, and improvement," *IEEE Trans. Ind. Inf.*, vol. 14, no. 7, pp. 3087–3096, Jul. 2018.

[22] D.-D. Mu, G.-F. Wang, and Y.-S. Fan, "Design of adaptive neural tracking controller for pod propulsion unmanned vessel subject to unknown dynamics," *J. Electr. Eng. Technol.*, vol. 12, no. 6, pp. 2365–2377, Nov. 2017.

[23] N. Wang and M. J. Er, "Direct adaptive fuzzy tracking control of marine vehicles with fully unknown parametric dynamics and uncertainties," *IEEE Trans. Control Syst. Technol.*, vol. 24, no. 5, pp. 1845–1852, Sep. 2016.

[24] S. Xingling and W. Honglun, "Back-stepping active disturbance rejection control design for integrated missile guidance and control system via reduced-order ESO," *ISA Trans.*, vol. 57, pp. 10–22, Jul. 2015.

[25] J. Yao and W. Deng, "Active disturbance rejection adaptive control of uncertain nonlinear systems: Theory and application," *Nonlinear Dyn.*, vol. 89, no. 3, pp. 1611–1624, Aug. 2017.

[26] J. Yao, Z. Jiao, and D. Ma, "Extended-state-observer-based output feedback nonlinear robust control of hydraulic systems with backstepping," *IEEE Trans. Ind. Electron.*, vol. 61, no. 11, pp. 6285–6293, Nov. 2014.

[27] X. L. Shao and H. Wang, "Attitude control of hypersonic vehicle based on SMDO-TLC," *J. Beijing Univ. Aeronaut. Astronaut.*, vol. 40, no. 11, pp. 1568–1575, Nov. 2014.

[28] X. Shao and H. Wang, "Sliding mode based trajectory linearization control for hypersonic reentry vehicle via extended disturbance observer," *ISA Trans.*, vol. 53, no. 6, pp. 1771–1786, Nov. 2014.

[29] W. He, Y. Dong, and C. Sun, "Adaptive neural impedance control of a robotic manipulator with input saturation," *IEEE Trans. Syst., Man, Cybern., Syst.*, vol. 46, no. 3, pp. 334–344, Mar. 2016.

[30] D. Mu, G. Wang, Y. Fan, B. Qiu, and X. Sun, "Adaptive course control based on trajectory linearization control for unmanned surface vehicle with unmodeled dynamics and input saturation," *Neurocomputing*, to be published, doi: 10.1016/j.neucom.2018.09.015.

[31] T. I. Fossen, *Handbook of Marine Craft Hydrodynamics and Motion Control*. 2011.
[32] M. Breivik, V. E. Hovstein, and T. I. Fossen, "Straight-line target tracking for unmanned surface vehicles," *Model., Identificat. Control, Norwegian Res. Bull.*, vol. 29, no. 4, pp. 131–149, 2008.
[33] H. K. Khalil, *Nonlinear Systems*. New York, Upper Saddle River, NJ, USA: Prentice-Hall, 1996.
[34] X. Shao and H. Wang, "A novel method of robust trajectory linearization control based on disturbance rejection," *Math. Problems Eng.*, vol. 2014, Apr. 2014, Art. no. 129247.
[35] X. Shao and H. Wang, "Trajectory linearization control based output tracking method for nonlinear uncertain system using linear extended state observer," *Asian J. Control.*, vol. 18, no. 1, pp. 316–327, Jan. 2016.
[36] M. C. Mickle and J. J. Zhu, "Nonlinear missile planar autopilot design based on PD-spectrum assignment," in *Proc. 36th IEEE Conf. Decis. Control*, vol. 4, Dec. 1997, pp. 3914–3919.
[37] J. J. Zhu, "PD-spectral theory for multivariable linear time-varying systems," in *Proc. 36th IEEE Conf. Decis. Control*, vol. 4, Dec. 1997, pp. 3908–3913.
[38] G. A. Anastassiou, "Fractional neural network approximation," *Comput. Math. Appl.*, vol. 64, no. 6, pp. 1655–1676, Sep. 2012.
[39] D. Mu, G. Wang, Y. Fan, X. Sun, and B. Qiu, "Adaptive LOS path following for a podded propulsion unmanned surface vehicle with uncertainty of model and actuator saturation," *Appl. Sci.-Basel.*, vol. 12, no. 7, p. 1232, 2017.
[40] Z. Zheng and Y. Zou, "Adaptive integral LOS path following for an unmanned airship with uncertainties based on robust RBFNN backstepping," *ISA Trans.*, vol. 65, pp. 210–219, Nov. 2016.
[41] L. Liu, D. Wang, and Z. Peng, "Path following of marine surface vehicles with dynamical uncertainty and time-varying ocean disturbances," *Neurocomputing*, vol. 173, pp. 799–808, Jan. 2016.
[42] P. Yan, D. Liu, D. Wang, and H. Ma, "Data-driven controller design for general MIMO nonlinear systems via virtual reference feedback tuning and neural networks," *Neurocomputing*, vol. 171, pp. 815–825, Jan. 2016.
[43] B. Chen, X. Liu, K. Liu, and C. Lin, "Direct adaptive fuzzy control of nonlinear strict-feedback systems," *Automatica*, vol. 45, no. 6, pp. 1530–1535, 2009.
[44] M. Chen, S. S. Ge, and B. Ren, "Adaptive tracking control of uncertain MIMO nonlinear systems with input constraints," *Automatica*, vol. 47, no. 3, pp. 452–465, Mar. 2011.
[45] J. Han, "From PID to active disturbance rejection control," *IEEE Trans. Ind. Electron.*, vol. 56, no. 3, pp. 900–906, Mar. 2009.
[46] J. Du, L. Wang, and C. Jiang, "Nonlinear ship trajectory tracking control based on backstepping algorithm," *Ship Eng.*, vol. 32, no. 1, pp. 41–44, 2010.
[47] X. Zhang, P. Shen, and Y. Bi, "Adaptive dynamic surface sliding mode control for ship trajectory tracking with disturbance observer," *Ship Eng.*, vol. 40, no. 7, 2018.
[48] S.-L. Dai, C. Wang, and F. Luo, "Identification and learning control of ocean surface ship using neural networks," *IEEE Trans. Ind. Informat.*, vol. 8, no. 4, pp. 801–810, Nov. 2012.
[49] C.-Z. Pan, X.-Z. Lai, S. X. Yang, and M. Wu, "An efficient neural network approach to tracking control of an autonomous surface vehicle with unknown dynamics," *Expert Syst. Appl.*, vol. 40, no. 5, pp. 1629–1635, 2013.
[50] J. Du, X. Hu, M. Krstić, and Y. Sun, "Robust dynamic positioning of ships with disturbances under input saturation," *Automatica*, vol. 73, pp. 207–214, Nov. 2016.

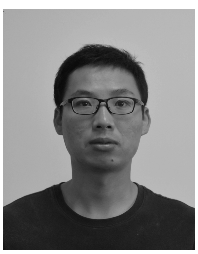

BINGBING QIU received the M.S. degree in control theory and engineering from Dalian Maritime University, Dalian, China, in 2017, where he is currently pursuing the Ph.D. degree in control theory and control engineering. His research interests include nonlinear control and intelligent control of unmanned surface vehicles.

GUOFENG WANG received the B.E., M.E., and Ph.D. degrees from Dalian Maritime University, Dalian, China, where he is currently a Professor with the School of Marine Electrical Engineering. He is also engaged in the technical research of marine automation system and automation equipment. He has presided over and participated in a number of national and ministerial projects. His research interests include ship automation, advanced ship borne detection device, and advanced power transmission.

YUNSHENG FAN received the B.E., M.E., and Ph.D. degrees from Dalian Maritime University, Dalian, China, in 2004, 2007, and 2012, respectively. He is currently an Associate Professor with the School of Marine Electrical Engineering, Dalian Maritime University. His research interests include ship intelligent control and its application.

DONGDONG MU received the M.S. degree in control theory and engineering from Dalian Maritime University, Dalian, China, in 2015, where he is currently pursuing the Ph.D. degree in control theory and control engineering. His research interests include modeling and intelligent control of unmanned surface vehicles.

XIAOJIE SUN received the M.E. degree in control engineering from Dalian Maritime University, Dalian, China, in 2016, where he is currently pursuing the Ph.D. degree in control theory and control engineering. His research interests include modeling and collision avoidance control of unmanned surface vehicles.